Patch-based DTI grading: Application to Alzheimer's disease classication

Kilian Hett, Vinh-Thong Ta, Rémi Giraud, Mary Mondino, José Manjón, Pierrick Coupé

Patch-based DTI grading: Application to Alzheimer's disease classification

Kilian Hett[1,2], Vinh-Thong Ta[1,2,3], Rémi Giraud[1,2,4,5], Mary Mondino[1,2], José V. Manjón[6], and Pierrick Coupé[1,2] and the Alzheimer's Disease Neuroimaging Initiative*

[1] Univ. Bordeaux, LaBRI, UMR 5800, PICTURA, F-33400 Talence, France
[2] CNRS, LaBRI, UMR 5800, PICTURA, F-33400 Talence, France
[3] Bordeaux INP, LaBRI, UMR 5800, PICTURA, F-33600 Pessac, France
[4] Univ. Bordeaux, IMB, UMR 5251, F-33400 Talence, France
[5] CNRS, IMB, UMR 5251, F-33400 Talence, France
[6] Universitat Politècnia de València, ITACA, 46022 Valencia, Spain

Abstract. Early diagnosis is one of the most important challenges related to Alzheimer's disease (AD). To address this issue, numerous studies proposed biomarkers based on anatomical MRI. Among them, patch-based grading demonstrated state-of-the-art results when applied to T1-weighted MRI. In this work, we propose to use a similar framework on different diffusion parameters extracted from DTI. We also propose to use a fast patch-based search strategy to provide novel biomarkers for the early detection of AD. We intensively compare our new grading-based DTI features with basic MRI/DTI biomarkers and evaluate our method within a cross validation classification framework. Finally, we demonstrate that the proposed biomarkers obtain competitive results for the identification of the different stages of AD.

Keywords: Patch-based grading, Alzheimer's disease classification, DTI, DWI, Mild Cognitive Impairment

1 Introduction

Alzheimer's disease (AD) and its prodromal phase are the most prevalent neurodegenerative disorders for the elderly people. The neurodegeneration caused by AD leads to an irreversible decline of memory and cognition abilities. One of the most important challenges is to find relevant biomarkers that could help for early diagnosis and prognosis of AD. Such imaging biomarkers can make easier the design of clinical trials that would allow faster development of new therapies.

Over the last years, numerous works proposed new imaging biomarkers to perform early diagnosis of AD. Among them, MRI-based methods showed that

* Data used in preparation of this article were obtained from the Alzheimer's Disease Neuroimaging Initiative (ADNI) database (adni.loni.usc.edu). As such, the investigators within the ADNI contributed to the design and implementation of ADNI and/or provided data but did not participate in analysis or writing of this report. A complete listing of ADNI investigators can be found at: `http://adni.loni.usc.edu/wp-content/uploads/how_to_apply/ADNI_Acknowledgement_List.pdf`.

the atrophy of medial temporal lobes is one of the most predictive biomarker candidates [1]. The volume of hippocampus (HC) is now considered as an important biomarker for mild cognitive impairment (MCI), the early stage of AD. HC-based biomarkers demonstrated state-of-the-art performances in AD classification as shown in several extensive comparisons (*e.g.*, [2, 3]). Recently, advanced patch-based grading within HC or over the whole brain were explored and demonstrated competitive performance [4–7]. These studies showed that patch-based grading methods are able to detect subtle hippocampal alterations several years before diagnosis [8] and can be useful to perform differential diagnosis [9].

Besides anatomical MRI, the use of DTI has been proposed to detect the first signs of microstructure alterations. Microstructural modifications are considered to occur before the atrophy measured by anatomical MRI. Therefore, we assume that DTI could be used as an earlier biomarker. DTI-based studies showed modifications of diffusion parameters in AD patients for structures such as corpus callosum, fornix, cingulum, hippocampus [10–13]. Moreover, it has been shown that HC mean diffusivity (MD) increase is related to pathology evolution [14] and thus could be used as an efficient biomarker of AD. Recently, more advanced methods using brain connectivity have been proposed to better capture white matter alterations [15,16]. These studies showed that brain connectivity is modified in the earliest stages of the pathologies.

Contributions: In this paper, we propose to apply the grading-based framework [4] on the different diffusion parameters extracted from DTI for AD classification. To reduce the computational burden, a fast patch-based search strategy is involved in the proposed method. In this work, we propose to compare the performances of basic DTI-based hippocampal features (*e.g.*, mean MD) with hippocampal volume to demonstrate the efficiency of DTI biomarkers. Next, we study the performance of the proposed patch-based DTI grading compared to MRI grading. Finally, we demonstrate the efficiency of these new biomarkers to identify the different stages of AD.

2 Materials and Methods

2.1 Dataset

Data used in this work were obtained from the Alzheimer's Disease Neuroimaging Initiative (ADNI) dataset[1]. ADNI is a North American campaign launched in 2003 with aims to provide and test MRI, PET, clinical and neurological measures and other biomarkers. This dataset includes AD patients, MCI subjects and elderly controls (CN). Table 1 shows the distribution of the data for each group. The data include 60 CN, 110 MCI composed of 74 early mild cognitive impairment (eMCI), 36 late mild cognitive impairment (lMCI) and 48 AD.

[1] `http://adni.loni.ucla.edu`

Table 1. Dataset description

Characteristic / Group	CN	eMCI	lMCI	AD
Number of subjects	60	74	36	48
Age (years)	73.3 ± 5.9	72.9 ± 8.0	73.5 ± 6.7	75.2 ± 8.6
Gender (male/female)	31/29	45/29	22/14	28/20

Data acquisition: For all subjects a whole brain MRI scanning and diffusion weighted imaging (DWI) on 3 Tesla GE Medical Systems scanners at 14 sites across North America was collected using the same protocol[2]. The DWI scans were composed of 46 separate angles, 5 T2-weighted images with no diffusion sensitization (b0 images) and 41 DWI (b=1000s/mm^2). The DWI protocol was chosen to optimize the signal-to-noise ratio in a fixed scan time [17].

MRI processing: T1-weighted (T1w) images were processed using the volBrain system [18][3]. This system is based on an advanced pipeline providing automatic segmentation of different brain structures from T1w MRI. The preprocessing is based on: (a) a denoising step with an adaptive non-local mean filter [19], (b) an affine registration in the MNI space [20], (c) a correction of the image inhomogeneities [21], and (d) an intensity normalization [22]. Afterwards, MRI are segmented in the MNI space using non-local patch-based multi-atlas methods [23]. The obtained hippocampus are segmented with the EADC protocol [24] designed for AD studies.

DTI processing: The preprocessing of the DWI images is based on: (a) a denoising step with a LPCA filter [25], (b) a correction of the head motion using an affine registration, and (c) an affine and a non-rigid registration to the T1w MRI in the MNI space [20]. Afterwards, a single tensor model [26] is estimated at each voxel using the Dipy software [27][4]. Next, we estimate the fractional anisotropy (FA), the axial diffusivity (AxD), the radial diffusivity (RD) and the mean diffusivity (MD) within the hippocampus structure with a mask provided by the volBrain system. These measures correspond to: the degree of diffusion anisotropy for the FA, the longitudinal diffusivity along the axonal fibers for the AxD, the diffusivity orthogonal to the axonal fibers for the RD and the mean diffusivity level in the three spatial directions for the MD.

2.2 Proposed Method

It is known that AD impacts specific brain areas especially the hippocampus. It has been shown that the hippocampal atrophy estimated on anatomical T1w MRI can help to classify the different stages of AD. However, a deterioration

[2] `https://adni.loni.usc.edu/wp-content/uploads/2010/05/ADNI2_GE_3T_22.0_T2.pdf`
[3] `http://volbrain.upv.es`
[4] `http://nipy.org/dipy/`

of the microstructure should precede this atrophy measured with anatomical MRI. To capture these early alterations, we propose to apply the Scoring by Nonlocal Image Patch Estimator (SNIPE) [4] on DTI images. This patch-based method estimates a map of scores representing a CN/AD likeness that reflects the amount of anatomical alterations caused by AD. Previous works showed that SNIPE provides competitive results when applied on HC [6,8]. In this paper, we propose for each subject to apply SNIPE on MD, RD, AxD and FA maps as well as T1w images. To reduce the resulting computational burden, we use the Optimized PAtchMatch Label fusion (OPAL) method, which is a fast approximate of K-nearest neigbhors search strategy designed for large 3D template library. This approach enables to perform structure grading in few seconds. Therefore, we can quickly estimate grading maps for FA, MD, AxD and RD and T1w MRI. Finally, we use the mean scores within HC mask for each grading maps to identify the different stages of AD.

Fast patch-based grading: Contrary to SNIPE that computes the distance of all the patches in a neighborhood surrounding the position of the considered voxel, the used of the OPAL strategy enables to directly obtain the good approximated candidates. The patch surrounding each voxel is used to estimate the anatomical pattern similarity between the considered subject i and a training library of templates – denoted L – composed of CN and AD patients. Once the set of the closest patches K_i is obtained with OPAL, the estimation of the grading value g can be computed for each voxel x_i as follows:

$$g(x_i) = \frac{\sum_{x_{j,t} \in K_i} w(x_i, x_{j,t}) p_t}{\sum_{x_{j,t} \in K_i} w(x_i, x_{j,t})}, \tag{1}$$

where $w(x_i, x_{j,t}) = e^{-\frac{d(P(x_i), P(x_{j,t}))^2}{h^2}}$ is the weight assigned to p_t in the grading value estimation. p_t corresponds to the pathological status of the template t, the value -1 is affected to an AD patient and 1 to a CN subject. The weight function w depends on the similarity between the patch $P(x_i)$ and $P(x_{j,t})$ centered on the voxels x_i and $x_{j,t}$, respectively. This similarity is estimated with a distance measure d. We use $h = \min_{x_{j,t}} d(x_i, x_{j,t}) + \epsilon$, with $\epsilon \to 0$. For the T1w images, the distance between two patches is provided by a zero mean normalized sum of squared differences (ZNSSD) defined as:

$$ZNSSD\left(P\left(x_i\right), P\left(x_{j,t}\right)\right) = \left|\left| \frac{P(x_i) - \mu_{P(x_i)}}{\sigma_{P(x_i)}} - \frac{P(x_{j,t}) - \mu_{P(x_{j,t})}}{\sigma_{P(x_{j,t})}} \right|\right|_2^2, \tag{2}$$

where μ and σ are the mean and the unbiased standard deviation of the considered patch, respectively. The advantage of the ZNSSD is to compute a robust inter-patches distance while addressing the local inhomogeneities problem. Contrary to anatomical MRI, DTI is a quantitative imaging. To preserve the quantitative information provided by each diffusion map we use the sum of squared differences (SSD) defined as:

$$SSD\left(P\left(x_i\right), P\left(x_{j,t}\right)\right) = ||P(x_i) - P(x_{j,t})||_2^2, \tag{3}$$

Features extraction: Mean value of each DTI map is measured within the hippocampus masks provided by the volBrain system in the MNI space. The hippocampus masks are used to compute the average grading values. Since the features are correlated with age, we performed a correction as done in [28].

Validation framework: The classification process is performed in a leave-one-out cross validation procedure. A linear discriminant analysis (LDA) is used to classify each test subjects. The results of each experiment are compared in terms of area under curve (AUC) and accuracy (ACC). The AUC is estimated with the *a posteriori* probabilities provided by the LDA. We carried out several experiments: CN vs. AD, CN vs. MCI, AD vs. MCI and eMCI vs. lMCI.

Parameter settings: The grading method is computed with a training library of 80 subjects composed of 40 AD and 40 CN templates. For each voxel that belongs to the HC area 100 patches are extracted from the training templates. The patch size is set to 5×5×5 voxels.

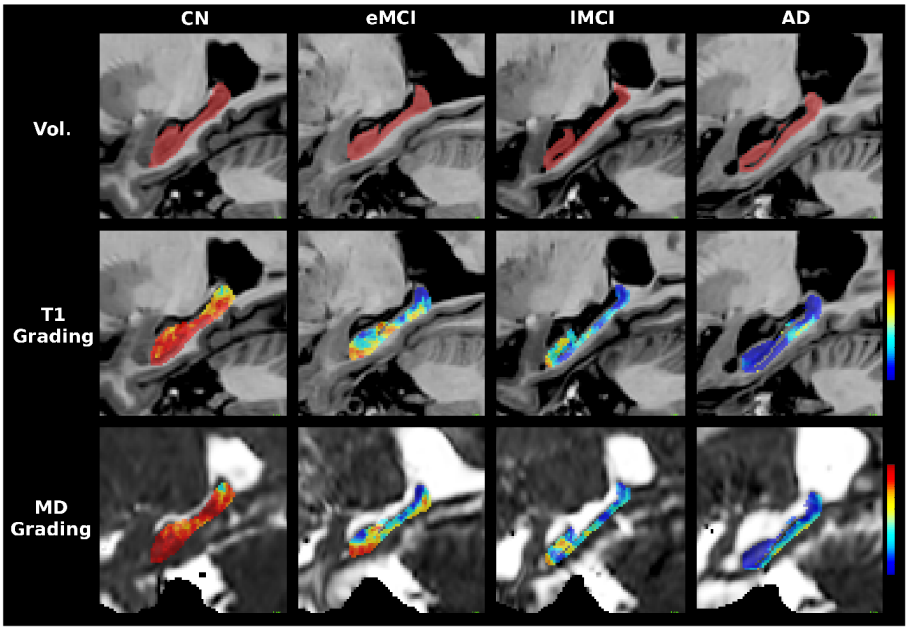

Fig. 1. From top to bottom: HC mask on the T1w images, T1w MRI grading and MD grading. For grading images blue and red colors correspond to the AD and the CN similarity, respectively.

Table 2. Comparison of the considered biomarkers. Underlined results correspond to the individual basic or grading based features. Bold-faced values correspond to the best ACC over all the features. The results of each column correspond to the AUC / ACC in percentage.

Features	CN vs. AD	CN vs. MCI	AD vs. MCI	eMCI vs. lMCI
Volume	88.4 / 83.1	69.5 / 63.9	71.1 / 67.2	67.2 / 63.7
Mean FA	64.2 / 59.2	57.7 / 56.1	54.0 / 52.7	38.2 / 43.1
Mean MD	85.7 / 80.3	66.0 / 62.6	75.0 / 72.5	67.6 / 62.8
Mean AxD	83.5 / 81.4	63.5 / 58.0	74.3 / 70.2	68.9 / 66.8
Mean RD	86.2 / 79.2	66.5 / 62.3	74.8 / 70.5	66.0 / 61.5
T1 Grading	**93.4 / 87.8**	**71.3 / 64.1**	82.0 / 73.4	68.7 / 66.2
FA Grading	85.0 / 80.1	63.5 / 60.1	74.9 / 70.3	63.0 / 60.7
MD Grading	90.6 / 86.5	68.8 / 60.7	80.4 / 76.3	70.4 / 65.8
AxD Grading	91.1 / 85.8	68.7 / 59.6	80.2 / 73.1	**71.8 / 67.6**
RD Grading	90.3 / 85.1	68.9 / 61.0	**80.0 / 76.5**	69.3 / 65.4

3 Results

Figure 1 shows the hippocampus segmentation, the T1 and MD grading maps for the considered groups. For the grading images, the blue and the red colors correspond to the AD and the CN similarity, respectively. As shown in Figure 1, grading values decrease in accordance to the different stages of AD and quantify impacts of the disease in each voxel. The T1w and MD grading maps show that for the CN subject, almost all the voxels are estimated as healthy while for the AD patient the majority of the voxels are detected to be impacted by AD. The results of the comparisons between basic biomarkers are summarized at the top of Table 2. HC volume provides the best accuracy for comparisons of CN vs. AD and CN vs. MCI with an ACC of 83.1% and 63.9%, an AUC of 88.4% and 69.5%, respectively. The DTI-based features provide best results for AD vs. MCI and eMCI vs. lMCI. For AD vs. MCI the mean MD provides 72.5% of ACC and 75% of AUC. For eMCI vs. lMCI the mean AxD provides 66.8% of ACC and 68.9% of AUC.

The lower part of Table 2 shows the results of the biomarkers based on grading. The grading-based biomarkers provide better results than the basic ones for all comparisons. The best result for the CN vs. AD is obtained by the T1w grading with 87.8% of ACC and 93.4% of AUC. The grading of this modality also provides the best results for the CN vs. MCI with an ACC of 64.1% and an AUC of 71.3%. The DTI-based grading features provide best ACC for AD vs. MCI and eMCI vs. lMCI. For AD vs. MCI the RD grading provides 76.5% of ACC and 80% of AUC. For eMCI vs. lMCI the MD grading provides 67.6% of ACC and 71.8% of AUC. It is interesting to note that results obtained with basic and grading-based features are in line. In fact, T1w-based features provide better results for AD vs. CN and CN vs. MCI while DTI-based features obtain better results for AD vs. MCI and eMCI vs. lMCI. These results demonstrate the interest of DTI-based features to analyze AD evolution along eMCI, lMCI and

AD stages. Recently, an advanced method based on brain connectivity has been evaluated on a similar dataset [16]. This approach obtained 78.5% of ACC for the CN vs. AD while MD grading obtains 86.5%. In addition, for the eMCI vs. lMCI, [16] obtained 63.4% while AxD grading obtains 67.6%. This demonstrates the competitive performance of the proposed DTI-based grading biomarkers.

4 Conclusion

In this work, we proposed a novel patch-based grading framework on different diffusion parameters extracted from DTI. The proposed method enables a fast feature extraction by using an optimized patch-based search strategy. We compare our new biomarkers with state-of-the-art MRI biomarkers and demonstrated that DTI grading provides efficient features for AD detection. Finally, we obtained competitive results to identify the different stages of AD. In a further work, we will study the complementarity of the grading based on T1w and DTI.

5 Acknowledgement

This study has been carried out with financial support from the French State, managed by the French National Research Agency (ANR) in the frame of the Investments for the future Program IdEx Bordeaux (ANR-10-IDEX-03-02), Cluster of excellence CPU and TRAIL (HR-DTI ANR-10-LABX-57) and the CNRS multidisciplinary project "Défi imag'In". This research was also supported by the Spanish grant TIN2013-43457-R from the Ministerio de Economia y competitividad, NIH grants P30AG010129, K01 AG030514 and the Dana Foundation.

References

1. Frisoni, et al.: The clinical use of structural MRI in Alzheimer disease. Nature Reviews Neurology **6**(2) (2010) 67–77
2. Cuingnet, et al.: Automatic classification of patients with Alzheimer's disease from structural MRI: a comparison of ten methods using the ADNI database. NeuroImage **56**(2) (2011) 766–781
3. Wolz, et al.: Multi-method analysis of MRI images in early diagnostics of Alzheimer's disease. PloS one **6**(10) (2011) e25446
4. Coupé, et al.: Scoring by nonlocal image patch estimator for early detection of Alzheimer's disease. NeuroImage: clinical **1**(1) (2012) 141–152
5. Liu, et al.: Ensemble sparse classification of Alzheimer's disease. NeuroImage **60**(2) (2012) 1106–1116
6. Tong, et al.: Multiple instance learning for classification of dementia in brain MRI. Medical image analysis **18**(5) (2014) 808–818
7. Komlagan, et al.: Anatomically constrained weak classifier fusion for early detection of Alzheimer's disease. In: MLMI, Springer (2014) 141–148
8. Coupé, et al.: Detection of Alzheimer's disease signature in MR images seven years before conversion to dementia: Toward an early individual prognosis. HBM **36**(12) (2015) 4758–4770

9. Koikkalainen, et al.: Differential diagnosis of neurodegenerative diseases using structural MRI data. NeuroImage: Clinical **11** (2016) 435–449
10. Rose, et al.: Gray and white matter changes in Alzheimer's disease: a diffusion tensor imaging study. Journal of Magnetic Resonance Imaging **27**(1) (2008) 20–26
11. Nir, et al.: Effectiveness of regional DTI measures in distinguishing Alzheimer's disease, MCI, and normal aging. NeuroImage: Clinical **3** (2013) 180–195
12. Wang, et al.: Interhemispheric functional and structural disconnection in Alzheimer's disease: a combined resting-state fMRI and DTI study. PloS one **10**(5) (2015) e0126310
13. Jung, et al.: Automated classification to predict the progression of Alzheimer's disease using whole-brain volumetry and DTI. Psychiatry investigation **12**(1) (2015) 92–102
14. Fellgiebel, et al.: Diffusion tensor imaging of the hippocampus in MCI and early Alzheimer's disease. Journal of Alzheimer's Disease **26**(s3) (2011) 257–262
15. Liu, et al.: Diffusion tensor imaging and tract-based spatial statistics in Alzheimer's disease and mild cognitive impairment. Neurobiology of aging **32**(9) (2011) 1558–1571
16. Prasad, et al.: Brain connectivity and novel network measures for Alzheimer's disease classification. Neurobiology of aging **36** (2015) S121–S131
17. Jahanshad, et al.: Diffusion tensor imaging in seven minutes: determining trade-offs between spatial and directional resolution. In: ISBI, IEEE (2010) 1161–1164
18. Manjón, et al.: volbrain: An online MRI brain volumetry system. In: Organization for HBM. (2015)
19. Manjón, et al.: Adaptive non-local means denoising of MR images with spatially varying noise levels. Journal of Magnetic Resonance Imaging **31**(1) (2010) 192–203
20. Avants, et al.: A reproducible evaluation of ANTs similarity metric performance in brain image registration. NeuroImage **54**(3) (2011) 2033–2044
21. Tustison, et al.: N4itk: improved n3 bias correction. IEEE transactions on medical imaging **29**(6) (2010) 1310–1320
22. Manjón, et al.: NICE: Non-local Intracranial Cavity Extraction. International Journal of Biomedical Imaging (2014)
23. Coupé, et al.: Patch-based segmentation using expert priors: Application to hippocampus and ventricle segmentation. NeuroImage **54**(2) (2011) 940–954
24. Boccardi, et al.: Training labels for hippocampal segmentation based on the EADC-ADNI harmonized hippocampal protocol. Alzheimer's & Dementia **11**(2) (2015) 175–183
25. Manjón, et al.: Diffusion weighted image denoising using overcomplete local PCA. PloS one **8**(9) (2013) e73021
26. Basser, et al.: MR diffusion tensor spectroscopy and imaging. Biophysical journal **66**(1) (1994) 259
27. Garyfallidis, et al.: Dipy, a library for the analysis of diffusion MRI data. Front. Neuroinform **8**(8) (2014)
28. Dukart, et al.: Age correction in dementia–matching to a healthy brain. PloS one **6**(7) (2011) e22193